Liquid-Vapour and Solid-Fluid Equilibria for the System Methane + Triacontane at High Temperature and High Pressure

J.J.B. Machado and Th. W. de Loos*

Delft University of Technology, Department of Chemical Technology, Physical Chemistry and Molecular Thermodynamics, Julianalaan 136, 2628 BL Delft, The Netherlands

Abstract

In this work experimental vapour-liquid and solid-fluid equilibrium data are presented for 13 different compositions of the system methane + triacontane. This data covers the temperature range from 315 K up to 450 K, and pressures up to 200 MPa. The compositions studied range from almost pure methane to pure triacontane. On the basis of the primary experimental two-phase equilibrium results, the course of the three-phase curve (solid triacontane + liquid + vapour) could be derived. The second critical end-point of this curve, where solid triacontane is in equilibrium with a critical fluid phase (s_{C30} + (l=g)) was found at T=(40.73±0.4) K, P=(128.55±0.5) MPa and a mole fraction in the critical fluid phase of x_{C30}=0.0275 ±0.002.

Keywords: vapour-liquid equilibria; solid-fluid equilibria; methane; triacontane; critical end-point; three-phase equilibria; hyperbaric reservoir fluids

* Corresponding author;
tel.: +31 15 278 8478; fax: +31 15 278 8713, e-mail: T.W.deLoos@tnw.tudelft.nl

Introduction

Recent developments in drilling technology allow the exploration of petroleum reservoirs at higher depths. Because of these higher depths these new reservoirs present peculiar characteristics regarding temperature, pressure and composition. It is possible to encounter reservoir temperatures up to 200 ºC, reservoir pressures up to 200 MPa, and a very asymmetric fluid composition, with mole fractions of methane up to 0.6 and the presence of long chain n-alkanes reaching up C60. These new reservoirs are normally known as “hyperbaric reservoirs”.

Because of the asymmetric composition of the hyperbaric reservoir fluids it is common that precipitation of solid phases occurs upon exploration and production of these reservoir fluids. It is of major importance to be able to model the phase behaviour of such asymmetric fluids at such extreme conditions of pressure and temperature. To do this we need accurate experimental data on the phase behaviour of asymmetric systems to evaluate the performance of existing models, and to help the development of new models.

Binary mixtures of methane and a heavy n-alkane do not have strong molecular interactions. In spite of this, they show, as a consequence of the relatively large difference in molecular size of the two components, fairly non-ideal behaviour at elevated pressures. There is a systematic change in the phase behaviour of systems of methane with heavy alkanes with the increase of the carbon number of the heavy alkane. Using the classification of Van Konynenburg and Scott [1-3] we can find phase behaviour of type II for lower carbon numbers up to 5. From carbon numbers of 6 until 10 type IV is the most likely to be found. Mixtures of methane with heavy n-alkanes with carbon number higher than 10 will show phase behaviour of type III with a metastable liquid-liquid phase split [4].

A complete description of a type III phase diagram with metastable liquid-liquid equilibria can be found elsewhere [6]. Here, we will give a short description of this type of type III phase behaviour, which is characterised by the existence of two branches of the three-phase curve solid heavy alkane + liquid + vapour. Both branches end in a critical endpoint where equilibrium is found between the solid heavy n-alkane and a critical fluid phase. The low-temperature branch of the three-phase curve starts at a quadruple point, and runs at a pressure just below the vapour pressure curve of pure methane, until it intersects the vapour-liquid critical curve in the first critical end point.

The second branch of the three-phase curve is found at higher temperatures, where it starts in the triple point of the pure heavy n-alkane and, runs to higher pressures until it intersects the vapour-liquid critical curve again in the second critical endpoint. As the pressure increases this branch of the three-phase curve first runs in many cases to lower temperatures and after passing trough a temperature minimum it runs to higher temperatures. This can be explained as the result of a competition between increasing melting point depression resulting from a higher methane solubility at high pressure and the increase of the melting temperature of the n-alkane with increasing pressure.

In this type of type III phase behaviour the three-phase curve liquid-liquid-vapour is metastable with respect to the appearance of an n-alkane solid phase. This type of type III phase behaviour is schematically shown Figure 1.

Examples of this type of type III phase behaviour were found by Glaser et al. [7] for the system methane + hexadecane, by van der Kooi et al. [4] for the system methane + eicosane and by Flöter et al. [6] for the system methane + tetracosane.

In this paper the results of an experimental investigation on the phase behaviour of the binary system methane + triacontane are presented

Experimental

The vapour-liquid, solid-liquid or -vapour, and solid-liquid-vapour equilibria for the system methane + triacontane were studied for 13 different compositions from almost pure methane to pure n-alkane. The temperature range investigated was from 330 K to 470 K, while the pressures did not exceed 200 MPa.

The methane used in this study was of ultra high purity (99.995 per cent w/w), supplied by Air Products. The triacontane was supplied by Sigma had a stated purity of >99 per cent w/w. All chemicals were used without any further purification.

Depending on the composition of the methane + triacontane mixture two different types of equipment were used. For pressures lower than 15 MPa a so-called Cailletet apparatus was used, while for higher pressures a windowed autoclave was used. In both cases, a sample of well-known composition is placed inside a half-open glass tube. The open side of the sample tube is emerged in mercury that serves both as a sealing fluid and as a pressure transmitting fluid. The phase transitions in the samples were measured visually.

The major differences between the two types of equipment are the pressure container and the way the temperature is controlled. In the Cailletet apparatus [9] the glass sample vessel is, itself, the pressure container. In this case, the temperature is controlled by immersing the glass vessel in a thermostated silicon oil bath, with temperature fluctuations not exceeding 0.04 K. In the case of the autoclave [10], since the pressures are much higher, the glass sample tube is placed inside an autoclave with two windows, and surrounded by pressurized water. The autoclave is placed in a thermostated air bath, with temperature fluctuations not exceeding 0.05 K. In both equipments a Pt-100 resistance thermometer is placed close to the glass vessel. The Pt-100 resistance is connected to a resistance bridge (ASL F-16) witch allows an accuracy of the temperature measurements of ±0.01K.

In both equipments the pressure measurements were made using a dead-weight gauge. In the Cailletet setup a dead-weight gauge (Budenberg “high ranger”) was used with accuracy better than ±0.003 MPa from 0.2 MPa to 5.61 MPa and ±0.05 MPa from 2.1 MPa to 15.0 MPa. In the autoclave setup the dead weight gauge (Tradinco “T 3800/1”) used allows accuracies better than ±0.04% of the reading from 3.0 MPa to 200.0 MPa.

A more detailed description of the equipment as well as the sample preparation procedure can be found elsewhere [4]. The uncertainties in the composition were not bigger than ±0.005 in mole fraction and had a tendency to decrease with decreasing the mole fraction of triacontane.

The actual determination of the phase boundaries involved the visual observation of the disappearing of a phase. In the case of the vapour-liquid equilibria we would start in the two-phase region and, keeping the temperature constant, slowly increase the pressure until we reach a homogeneous state. This would be a vapour phase when we are on the dew point side and a liquid phase if we were working on the bubble point side. This kind of procedure, taking in account the visual limitations, allows determining the vapour-liquid boundary curve, for a certain composition, with an accuracy better than ±0.075 MPa for bubble points, and ±0.12 MPa for dew points. For the determination of the solid-fluid equilibria we started in the two-phase region solid + fluid and, keeping the pressure constant, slowly increase the temperature until we reach the homogeneous phase. These measurements have accuracy better than ±0.25 K in temperature.

Points of the three phase curve, solid triacontane + liquid + vapour, were determined in an indirect way. For a certain composition the solid-fluid curve and the liquid-vapour curve are almost perpendicular to each other. This allows the

determination of a three-phase point by the intersection of these two curves. The achieved uncertainties for the three-phase points were less than ±0.3 MPa in pressure and ±0.15 K in temperature.

Results

For 13 different compositions of mixture of methane and triacontane the liquid-vapour and solid-fluid equilibria was determined, allowing a clear insight in the phase behaviour of this asymmetric system. These measurements are presented in table 1, with a notation of "dp" for compositions with dew-point behaviour and "bp" for curves with bubble-point behaviour. In table 2 the data for the solid-fluid equilibria are presented.

Using the primary isoplethic experimental data and low degree polynomial fits it was possible to derived isobaric and isothermal cross sections by interpolation. The resulting (P, x) diagrams for the vapour-liquid equilibria are represented in figure 2 for T=353.15K, T=373.15 K and T=423.15 K. In figure 2 the same isobaric data are also plotted using hard-core volume fractions as composition variable instead of mole fractions. These volume fractions were calculated using the Van der Waals volumes according to Bondi [5]. The use of volume fractions instead of mole fractions helps to have a more symmetric depiction of vapour-liquid two-phase region.

It can be seen from figure 2 that with increasing temperature, the pressure of the vapour-liquid equilibria decreases. The bubble-point pressure is a strong function of the mole fraction of triacontane. The figure also shows that the critical composition of the vapour-liquid equilibria does not change too much in the temperature range investigated. The variation of the critical composition from 350 K to 450 K is less than 0.004 in mole fraction. The critical pressure varies from 117.1 MPa at T=353.15 K to 91.0 MPa at T=423.15 K. These high values for the critical pressure are typical for asymmetric systems. This behaviour was also found for the system methane-eicosane [4] and for the system methane-tetracosane [6]. The critical composition is x_{C30}=0.0225±0.003 or in terms of hard core volume fraction equal to 0.296±0.03.

In figure 3 the isobaric solid-fluid cross sections obtained from interpolations of the experimental data are presented. At constant composition the solidification temperatures of the system decreases systematically with decreasing the pressure. At constant pressure the solidification temperature increases with increasing mole fraction of triacontane, up to the melting point of pure triacontane.

If we take the coordinates of the three-phase points of two different samples with composition close to each other and in the vicinity of the composition of the second critical endpoint, one showing dew-point behaviour and the other showing bubble-point behaviour, the composition of the critical fluid phase present in the second critical endpoint lays between the compositions of the two samples chosen. If the samples do not differ to much in their composition the coordinates of their three-phase points do not differ too much, because both the (P,x) and the (T,x) projections of the three-phase curves show a relatively flat local maximum for the composition of the fluid phase at the second critical endpoint. This allows us to determine the coordinates of the second critical endpoint. The coordinates for the second critical end-point were T=(40.73±0.15) K, P=(128.55±0.25) MPa and x_{C30}=(0.0275±0.0012).

The three-phase points presented in table 3 and represented in figure 4 together with the same type of three-phase data for the systems methane + hexadecane [7], methane + eicosane [4] and methane + tetracosane [6]. Flöter et al. [8] measured the coordinates for the second critical endpoint for different methane + heavy n-alkane systems. For the system methane + triacontane they found for the second critical endpoint T=(340.6±0.4) K, P=(124.2±0.5) MPa and x_{C30} =0.0305±0.002. It

can be concluded that the data presented in this work agrees well with the literature data.

Discussion

For the system methane + triacontane vapour-liquid and solid-fluid equilibria were measured. Using these data the three-phase curve solid triacontane + liquid + vapour was determined. As found by other authors [4,6,7] also this system fits in the systematic behaviour of methane + n-alkane mixtures, showing type III phase behaviour with metastable liquid-liquid-vapour equilibria. This systematic behaviour can be seen in figure 4 where the three-phase curves solid-liquid-vapour for different methane + n-alkane systems is plotted. It was found that the three-phase curve for these kind of systems presents a minimum in temperature, and that this minimum occurs more or less for the same pressure: P=(30±5)MPa.

Besides this still unexplained fact, also the composition at this temperature minimum is almost the same for all the systems investigated: $x_{C16} \approx x_{C20} \approx x_{C24} \approx x_{C30} \approx$ (0.35±0.05). In the case of the system studied here the temperature at this minimum was found at T=(333.67±0.3) K. The temperature at this minimum increases as the carbon number of the heavy alkane increases. Also the effects of the asymmetric nature of these binary systems are more pronounced as we increase the chain length of the heavy alkane. The increase of the chain length of the heavy n-alkane shifts the fluid-phase boundaries to higher temperatures and higher pressures. This can be seen in figure 4.

In figure 5 the temperatures and pressures of the second critical end-point for different methane + n-alkane systems are plotted as function of the carbon number of the heavy alkane. The data, besides the one presented in this work for the system methane + triacontane, plotted was obtained from literature [8]. We can see that both the temperature and the pressure increase, in a more or less linear way, when the length of the heavy alkane increases. The increase in the temperature can be easily explained by the increase in the melting point of the pure alkane with increasing chain length. An increase of the chain length of the heavy alkane will reduce its solubility in the critical phase allowing the extension of the vapour-liquid envelops to higher pressures.

References

1. Van Konynenburg, P.H. Ph.D. thesis, UCLA **1968**.
2. Scott, R.L.; Van Konynenburg, P. H. Disc. Faraday Soc., 49 (1970**)**, ,87.
3. Van Konynenburg, P. H.; Scott, R.L. Phil. Trans. Roy. Soc. Lond., A298 (1980**)** 495.
4. Van der Kooi, H.J.; Flöter, E.; De Loos, Th. W.; J. Chem. Thermodyn.,, 27 (1995) 847
5. Bondi, A.; Physical Properties of Molecular Crystals, Liquids and Gases; Wiley, New York, 1968.
6. Flöter, E.; De Loos, Th. W.; de Swaan Arons, J.; Fluid Phase Equilib., 127 (1997) 129.
7. Glaser, M.; Peters, C.J.; Van der Kooi, H.J.; Lichtentaler,R.N.; J. Chem. Thermodyn., 17 (1995) 803.
8. Flöter, E.; De Loos, Th. W.; Int. J. Thermophys., 16 (1995), 185.
9. De Loos, Th, W.; Van der Kooi, H.J.; Ott, P. L.; J. Chem. Eng. Data 31, (1986), 166
10. De Loos,Th, W. ; Wijen, A.J.M.; Diepen, G.A.M.; J. Chem. Thermodyn., 12 (1980) 193.

Figure 1: Schematic phase behaviour of asymmetric binary methane + n-alkane systems with type III phase behaviour. Symbols: ○, pure component critical point; Δ pure component triple point; ▲ critical endpoint; □ quadruple point. Lines: _____, pure component phase curve; ……, metastable equilibria; -.-.-.-.-.-, three phase line; ———, critical curve.

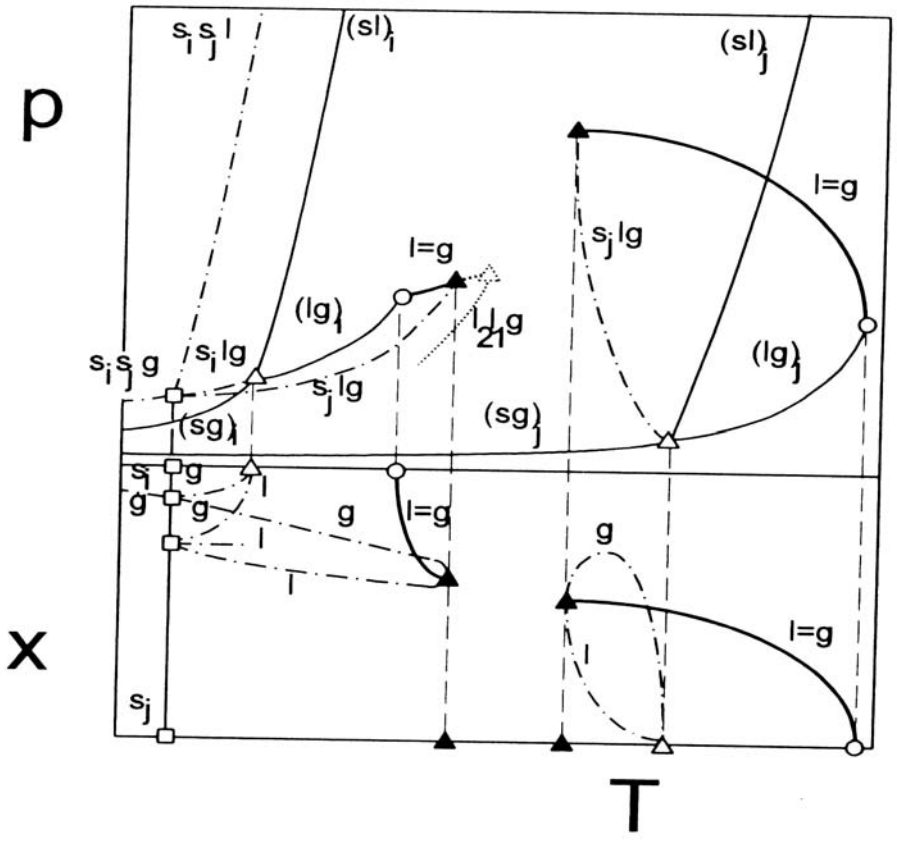

Figure 2: Isothermal vapour-liquid equilibria for the system methane+ - triacontane. Bubble- and dew-point pressure as function of mole fraction (open symbols) or volume fraction (filled symbols). Data obtained by interpolation of experimental data using low degree polynomial fittings.

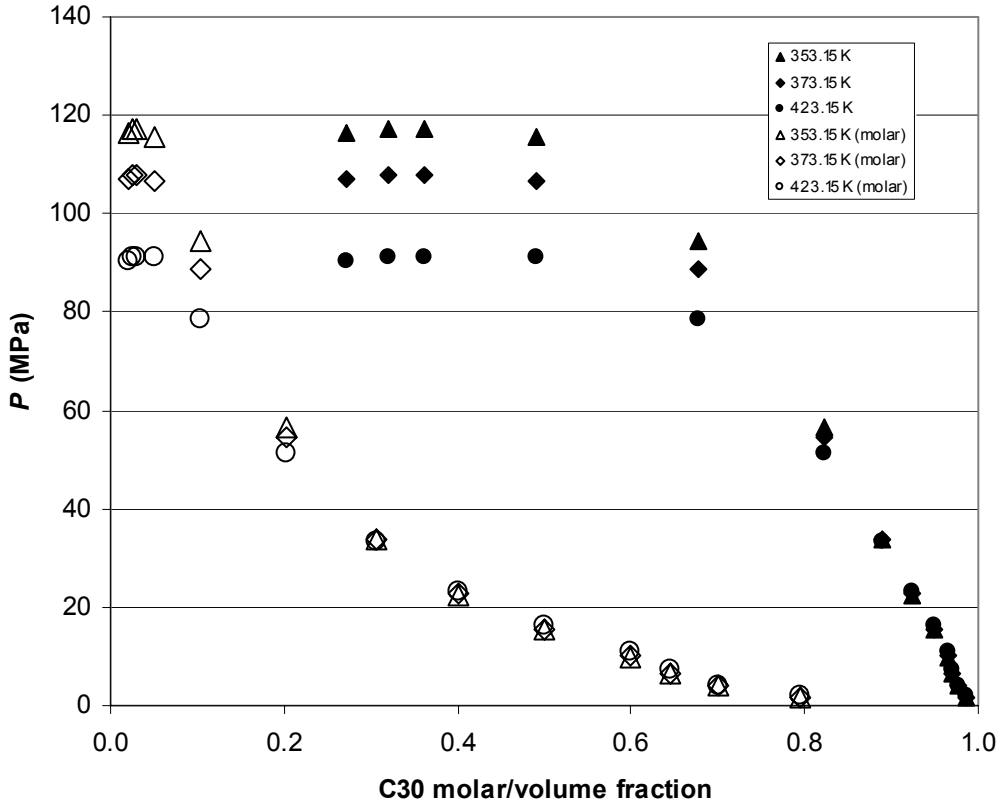

Figure 3: Isobaric solid-fluid equilibria for the system (1-*x*) methane + *x* triacontane. Data obtained from low degree polynomial fits of the experimental isophletic data.

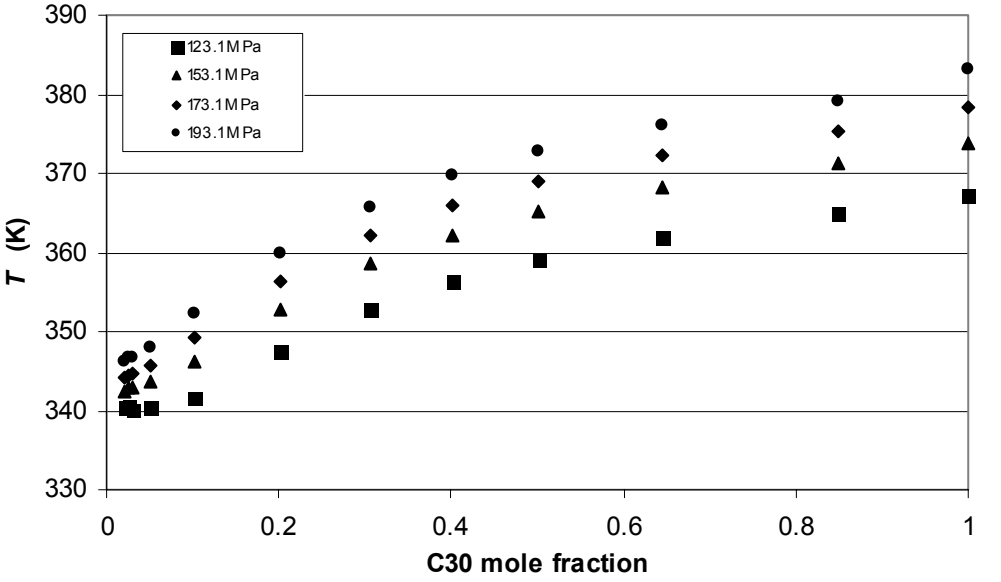

Figure 4: Three-phase curves solid heavy alkane + liquid + vapour for different methane-heavy n-alkane systems. ●, second critical endpoint.

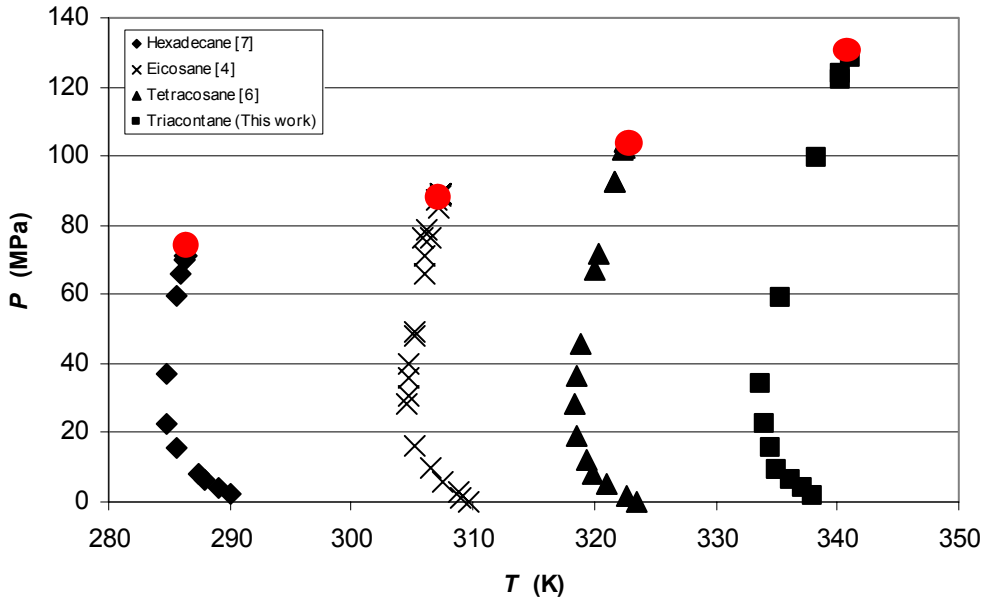

Figure 5: Coordinates of the second critical endpoint as function of carbon number for different methane-heavy n-alkane systems (*For references see text*).

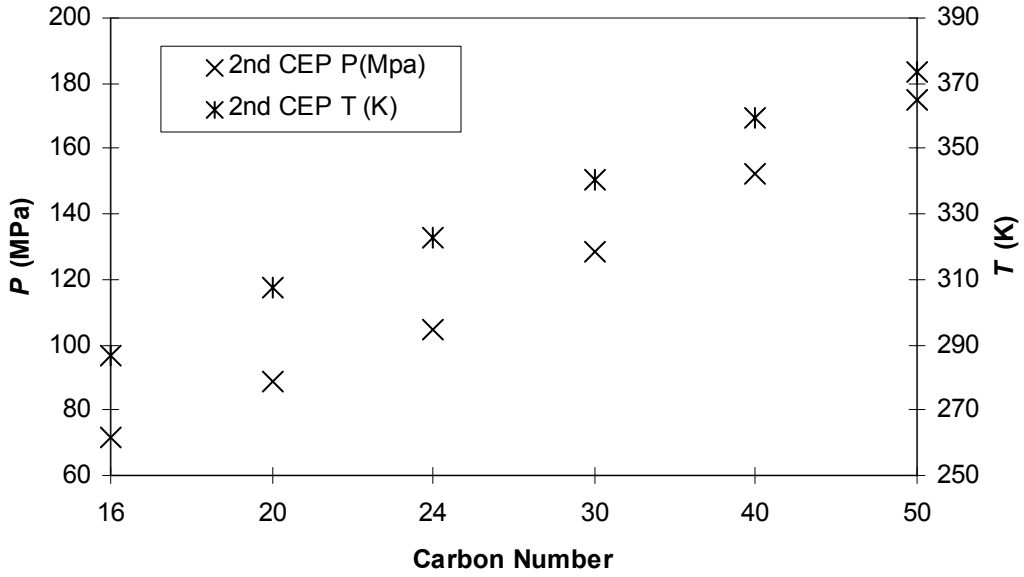

Table 1. Vapour-liquid equilibria for the system (1-*x*)-methane + *x*-triacontane: bubble- or dew-point pressure as function of temperature *T* at a given mole fraction x of triacontane.

x=0.020 (dp)		*x*=0.025 (dp)		*x*=0.030 (bp)		*x*=0.050 (bp)		*x*=0.103 (bp)	
T (K)	*P* (MPa)	*T* (K)	*P* (MPa)	*T* (K)	*P* (MPa)	*T* (K)	*P* (MPa)	*T* (K)	*P* (MPa)
340.94	123.40	345.36	121.20	350.07	118.90	351.46	116.40	340.52	98.70
350.43	117.90	355.08	116.10	359.46	114.20	360.30	112.20	349.65	95.50
359.88	113.10	364.85	111.40	369.04	109.30	369.67	108.20	359.07	92.70
369.33	108.80	374.05	107.50	377.72	106.20	378.78	104.60	368.96	89.70
378.54	105.00	383.03	103.90	386.79	103.00	388.33	101.20	377.90	87.50
387.93	101.50	392.47	100.50	396.32	99.50	397.81	98.20	387.16	85.40
396.96	98.40	402.06	97.40	404.99	96.70	407.36	95.30	396.58	83.40
406.35	95.40	411.20	93.70	414.65	93.80	416.71	92.80	405.95	81.60
415.72	92.50	420.93	91.80	424.12	91.30	426.16	90.20	415.13	80.00
425.33	89.80	430.24	89.30	433.38	88.80	435.40	88.10	424.36	78.30
435.07	87.50	439.59	86.90	442.94	86.30	444.50	85.70	433.78	76.70
443.74	85.00	448.52	84.70	450.87	84.40	453.76	83.40	443.07	75.20
452.90	82.80	458.61	82.20	460.77	82.20	462.97	81.40	452.38	73.70
462.35	80.40	467.45	80.20	470.68	79.90	472.48	79.40	461.62	72.40
471.25	78.30							470.63	71.00

Table 1. *Continued*

x=0.202 (bp)		*x*=0.307 (bp)		*x*=0.402 (bp)		*x*=0.500 (bp)		*x*=0.598 (bp)	
T (K)	*P* (MPa)	*T* (K)	*P* (MPa)	*T* (K)	*P* (MPa)	*T* (K)	*P* (MPa)	*T* (K)	*P* (MPa)
341.27	57.90	338.09	33.90	341.22	22.40	345.85	15.30	352.09	9.91
341.27	57.90	350.51	33.80	369.59	22.70	355.23	15.40	362.34	10.10
350.80	56.80	360.06	33.70	378.48	22.80	364.80	15.50	372.42	10.29
360.30	55.70	369.99	33.60	388.04	22.90	373.39	15.60	382.46	10.42
365.04	55.20	378.64	33.60	397.67	23.00	382.82	15.70	392.49	10.56
370.50	54.90	388.09	33.50	407.15	23.10	392.44	15.80	402.48	10.68
374.93	54.50	397.41	33.40	416.52	23.10	402.35	15.90	412.49	10.78
379.50	54.10	406.78	33.30	425.97	23.20	411.84	16.00	422.36	10.87
384.51	53.70	416.44	33.20	435.29	23.30	421.31	16.10	432.54	10.94
389.23	53.30	428.49	33.10	444.98	23.30	430.53	16.20	442.38	11.00
393.93	53.00	444.26	33.00	454.95	23.30	449.46	16.50	452.34	11.03
398.56	52.70	453.87	32.80	461.75	23.40	459.15	16.70	462.35	11.08
403.27	52.40	463.24	32.60	472.29	23.50				
408.07	52.10	472.26	32.40						
412.77	51.90								
417.45	51.60								

422.25	51.40
426.76	51.10
431.35	50.80
436.06	50.50
440.78	50.20
445.56	49.90

Table 1. *Continued*

x=0.701 (bp)		*x*=0.794 (bp)		*x*=0.901 (bp)	
T (K)	*P* (MPa)	*T* (K)	*P* (MPa)	*T* (K)	*P* (MPa)
342.07	6.52	342.20	3.86	342.77	1.64
352.01	6.60	352.27	3.90	347.71	1.65
362.00	6.63	360.40	3.95	357.96	1.70
372.19	6.69	362.40	3.98	367.97	1.73
382.35	6.74	370.50	4.04	377.88	1.76
392.36	6.83	372.50	4.05	387.75	1.79
402.37	7.00	381.42	4.15	397.59	1.82
412.52	7.11	397.72	4.26	407.59	1.84
422.38	7.20			417.70	1.87
432.38	7.26			427.66	1.89
442.41	7.33			437.70	1.91
442.41	7.39			447.61	1.93
457.09	7.42			457.64	1.94
472.50	7.48			467.64	1.96

Table 2. Solid-fluid equilibria for the system (1-*x*) methane + *x* triacontane: solidification pressure *P* as a function of temperature *T* at a given mole fraction *x*

x=0.02		*x*=0.025		*x*=0.03		*x*=0.05		*x*=0.103	
T (K)	*P* (MPa)	*T* (K)	*P* (MPa)	*T* (K)	*T* (K)	*P* (MPa)	*T* (K)	*P* (MPa)	*T* (K)
340.39	125.10	341.51	133.10	340.62	128.10	340.44	125.10	340.34	113.10
341.25	133.10	342.37	143.10	341.20	133.10	341.62	133.10	341.72	123.10
341.69	143.10	343.26	153.10	341.98	143.10	342.35	143.10	343.24	133.10
342.50	153.10	344.36	163.10	342.79	153.10	343.55	153.10	344.60	143.10
343.32	163.10	345.02	173.10	343.79	163.10	344.62	163.10	346.30	153.10
344.23	173.10	345.93	183.10	344.73	173.10	345.88	173.10	347.68	163.10
345.09	183.10	346.85	193.10	345.88	183.10	346.98	183.10	349.12	173.10
346.27	193.10			346.69	193.10	348.05	193.10	350.70	183.10

Table 2 - *Continued*

x=0.202		*x*=0.307		*x*=0.402		*x*=0.500		*x*=0.645	
T (K)	*P* (MPa)	*T* (K)	*P* (MPa)	*T* (K)	*P* (MPa)	*P* (MPa)	*T* (K)	*P* (MPa)	*T* (K)
337.43	70.10	338.14	53.10	339.00	43.10	335.25	18.10	346.30	53.10
339.28	80.00	340.34	63.10	341.30	53.10	336.68	23.10	348.52	63.10
341.14	90.00	342.61	73.10	343.89	63.10	338.98	33.10	350.88	73.10
341.37	91.20	344.57	83.10	346.09	73.10	341.43	43.10	353.08	83.10
343.04	100.00	348.81	103.10	347.89	83.10	343.81	53.10	355.39	93.10
344.90	110.00	350.85	113.10	350.17	93.10	346.17	63.10	357.62	103.10
346.19	116.70	353.15	123.10	352.16	103.10	348.34	73.10	360.06	113.10
346.84	120.00	354.66	133.10	354.47	113.10	350.46	83.10	362.14	123.10
348.75	130.00	356.55	143.10	356.28	123.10	352.64	93.10	364.06	133.10
350.48	140.00	358.46	153.10	358.49	133.10	354.79	103.10	365.98	143.10
352.29	150.00	360.43	163.10	360.46	143.10	357.18	113.10	368.17	153.10
354.00	160.00	362.19	173.10	362.40	153.10	359.01	123.10	370.04	163.10
		363.98	183.10	363.77	163.10	361.04	133.10	372.10	173.10
				366.14	173.10	363.30	143.10	374.29	183.10
						365.09	153.10		
						367.11	163.10		
						369.01	173.10		

Table 2. *Continued*

x=0.850		*x*=1.000	
T (K)	*P* (MPa)	*T* (K)	*P* (MPa)
349.65	53.10	344.47	23.10
351.85	63.10	346.90	33.10
353.90	73.10	351.80	53.10
356.07	83.10	356.39	73.10
358.20	93.10	360.67	93.10
360.35	103.10	365.11	113.10
365.06	123.10	370.46	133.10
371.30	153.10	374.52	153.10
373.26	163.10	378.67	173.10
375.21	173.10	382.29	193.10
377.16	183.10		
379.17	193.10		

Table 3. (Solid+liquid+vapour) three-phase points for the system methane + triacontane derived by interception of isoplethic (solid-fluid) and (vapour-liquid) boundary curves.

x_{C30}	T (K)	P (Mpa)	x_{C30}	T (K)	P (MPa)
0.02	340.28	123.68	0.3067	333.67	33.97
0.0250	341.08	128.62	0.4020	334.01	22.31
0.0300	340.35	124.06	0.5000	334.55	15.42
0.0500	340.21	122.09	0.5980	335.03	9.48
0.1030	338.33	99.45	0.7013	336.15	6.54
0.2020	335.40	58.72	0.7939	337.15	3.97